Multireference calculations of the phosphorescence and photodissociation of chlorobenzene

Ya-Jun Liu
Department of Quantum Chemistry, Uppsala University, Box 518, S-751 20 Uppsala, Sweden

Petter Persson
Department of Quantum Chemistry, Uppsala University, Box 518, S-751 20 Uppsala, Sweden and CALTECH, Beckman Institute 139-74, Materials and Process Simulation Center, Pasadena, California 91125

Sten Lunell[a)]
Department of Quantum Chemistry, Uppsala University, Box 518, S-751 20 Uppsala, Sweden

(Received 30 June 2004; accepted 7 September 2004)

Multireference complete active space self-consistent-field (CASSCF) and multireference CASSF second-order perturbation theory (MSCASPT2) calculations were performed on the ground state and a number of low-lying excited singlet and triplet states of chlorobenzene. The dual phosphorescence observed experimentally is clearly explained by the MSCASPT2 potential-energy curves. Experimental findings regarding the dissociation channels of chlorobenzene at 193, 248, and 266 nm are clarified from extensive theoretical information including all low-energy potential-energy curves. © *2004 American Institute of Physics.* [DOI: 10.1063/1.1810135]

I. INTRODUCTION

Aryl halides play an important role in chemical synthesis and are of practical significance to environmental protection.[1,2] The properties of their excited states have also received attention in both experimental[3–6] and theoretical[7–10] studies.

Takemura *et al.* observed dual phosphorescence of chlorobenzene (ClBz) in a rigid glass solution.[11] They confirmed that the dual phosphorescence consists of a broad peak with a maximum at about 480 nm and a somewhat structured peak with a maximum near 400 nm. The two features correspond to short-lived and long-lived emission, respectively. Their observed lifetimes are 3 ± 0.4 and 12 ± 2 ms, respectively.[11] They assigned the slow phosphorescence to a $S_0 \leftarrow T(\pi,\pi^*)$ transition, and the predominant fast phosphorescence to a $T(\pi,\sigma^*)$ state.[12] Nagaoka *et al.*[7] studied the low-lying triplet states of ClBz by Hartree–Fock (HF) calculations, and they assigned the slow phosphorescence to the transition from the first T-A_1 state to the S_0 state, and the fast phosphorescence to the transition from the second T-B_1 state to the S_0 state. Rubio-Pons *et al.*[13] calculated the lifetime of its lowest triplet state using the complete active space self-consistent-field (CASSCF) method. However, they did not provide high-quality potential-energy curves (PECs) for the ClBz ground and excited states. Here we present PECs of the ground and several low-lying excited singlet and triplet states from multireference CASSCF second-order perturbation theory[14] (MSCASPT2) calculations. These curves are important for clearly understanding the dual phosphorescence of ClBz. The interpretation of the experimental results in terms of two low-lying triplet states is further supported by the present calculations. This is one of the objectives of this work.

Experimentally, the photodissociation dynamics of ClBz has been studied at 266 nm by femtosecond pump-probe spectroscopy[5] and crossed laser-molecular-beam technique.[15] Experiments have also been published for excitations by an excimer laser at 248 (Ref. 16) and 193 nm.[16–18] It was concluded from these experimental studies that the photodissociation of the C–Cl bond in ClBz following a 193-nm excitation takes place through three different dissociation channels with probabilities of similar magnitudes. The first channel was assigned to a direct dissociation or very fast predissociation, the second channel is via vibrationally excited triplet levels, and the third dissociation channel is via highly excited vibrational levels of the ground electronic state (hot molecules). The photodissociation of ClBz at 248 nm was proposed to occur dominantly via the second and third of the above-mentioned channels. The photodissociation at 266 nm has been given alternative explanations. On one hand, it was proposed to be due to a hot molecule mechanism by Wang *et al.*[15] On the other hand, Kadi *et al.*[5] assigned it to the decay of an initially excited (π,π^*) state to a repulsive triplet (n,σ^*) state due to spin-orbit coupling, and they observed its time constant to be 1 ns.[5] The experimental explanation of the photodissociation channels of ClBz must thus, in many ways, still be regarded as tentative. For example, we still do not know if the first channel at 193 nm is due to direct dissociation or fast predissociation, or which specific states contribute to the photodissociation at the longer wavelengths.

High-quality calculated PECs can provide much useful information for a detailed understanding of the dissociation dynamics following excitation at a specific wavelength. The main objective of this paper is therefore to provide accurate

[a)]Author to whom correspondence should be addressed. Electronic mail: sten.lunell@kvac.uu.se

calculated PECs to enable a clear and detailed explanation of the photodissociation mechanism of ClBz at different wavelengths. Besides our recent theoretical study of the aryl halide photodissociations at 266 nm,[10] Nagaoka *et al.* calculated the PECs of some low-lying triplet states of ClBz by the HF method.[7] We have not found any calculated PECs of ClBz pertinent to the photodissociation experiments conducted at 248 and 193 nm, although it has been suggested that accurate calculations of higher excited electronic states could be useful to clarify experimental findings for ClBz.[19] Investigating a larger number of excited states allows us to consider changes in the photodissociation behavior for initial photoexcitations using higher-energy photons, adding another dimension to our recent aryl halide studies that focused on substitution effects for the low-energy photodissociation channels.[9,10] In these works, the MSCASPT2 method was used to calculate vertical excitation energies (T_v), and PECs of ground and excited states.

This paper is organized in such a way that we first describe the methods and results of the quantum-chemical calculations before broadening the discussion to comparisons with experimental observations and previous theoretical calculations on the phosphorescence and photodissociation of ClBz.

II. COMPUTATIONAL METHODS

Most calculations were performed using the MOLCAS 5.4 quantum-chemistry software.[20] Atomic natural orbital (ANO) basis sets[21] were used for all the atoms. C($10s6p3d$), H($7s3p$), and Cl($13s10p4d$) are contracted to ($3s2p1d$), ($2s1p$), and ($4s3p2d$), respectively. The second-order Moller–Plesset perturbation theory (MP2) (Ref. 22) method with the 6-311+G(d,p) basis set[23] was used to calculate basis set superposition error (BSSE) corrected energies. These calculations were carried out using the GAUSSIAN 03 program.[24] The results have been checked for BSSE, which was found to be of negligible importance in this case.

The geometries of the ground and excited states were optimized using the CASSCF method. MSCASPT2 methods were then used to calculate the vertical excitation energies (T_v) of the three lowest-lying singlet and triplet states of every irreducible representation in the C_{2v} symmetry of the molecule. That is to say, 12 singlet and 12 triplet states were calculated. Of course, these states are not necessarily the 24 overall lowest-lying states. The PECs along the reaction coordinate described by the Cl–C_6H_5 bond distance were calculated using the MSCASPT2 method for all these 24 states. The harmonic vibrational frequencies of the ground state were calculated using the CASSCF method. The same threshold and shift were used in the calculations of all the PECs. In the CASSCF calculations, 12 electrons were active. The active space included the six p orbitals of the phenyl ring, the σ and σ^* orbitals of the C_1–Cl bond, and the two remaining $3p$ orbitals of chlorine. The states average technique was used in the CASSCF T_v calculations. The $1s$ cores of carbon and chlorine were frozen in the CASPT2 calculations.

TABLE I. Calculated and experimental ground-state geometry of ClBz.

Method	CASSCF[a]	CASSCF[b]	RHF[c]	UHF[d]	Expt.[e]
R(Cl–C_1)	1.746	1.778	1.745	1.820	1.741
R(C_1–C_2)	1.403	1.392	1.383	1.374	1.393
R(C_2–C_3)	1.399	1.395	1.385	1.385	1.396
R(C_3–C_4)	1.399	1.387	1.385	1.384	1.401

[a]The present paper.
[b]Reference 10.
[c]Reference 15.
[d]Reference 7.
[e]Reference 25.

III. RESULTS

A. Ground state

We used the CASSCF method to optimize the ground-state geometry of ClBz. The present result, the previous reported calculated results,[7,10,15] and the corresponding experimental fitted values[25] are listed in Table I. We also optimized the ground-state geometry of ClBz by CASSCF in Ref. 10. Due to the use of an effective core potential basis set on the Cl atom in Ref. 10, the optimized Cl–C_1 bond distance (1.778 Å) differs a little more from the experimental fitted value (1.742 Å). Cl is not a very heavy atom, so we used an ANO basis set here to get a better optimized geometry. From Table I, the CASSCF optimized ground-state geometry is seen to agree very well with the corresponding experimental fitted values.

The frequencies of the ClBz ground state have previously been calculated by the Becke–3-Lee–Yang–Parr, MP2, and CASSCF methods,[26] and the HF method.[27] However, as the symmetries of the vibrational modes were not indicated in Ref. 26, we only compare the present CASSCF calculated result with the HF results in Ref. 27 and the experimental results; see Table II. The present CASSCF calculated vibrational ground-state frequencies agree well with the experiment both in magnitude and in the assignment of the vibrational modes.[28–30]

B. Vertical excitation energies

The MSCASPT2 method was used to calculate the vertical excitation energy, T_v, of the three lowest-lying singlet and triplet states of every irreducible representation in the C_{2v} symmetry of ClBz at its CASSCF optimized ground-state geometry. From the calculated results, we determined the seven lowest singlet and six lowest triplet states of ClBz to be S_0-A_1, S_1-B_2, S_2-A_1, S_3-B_2, S_4-B_1, S_5-A_2, and S_6-A_1, and T_1-A_1, T_2-B_2, T_3-A_1, T_4-B_2, T_5-B_1, and T_6-A_1, respectively; see Table III. For ease of notations, the other calculated five singlet and six triplet states are also denoted using consecutive subscript numbers in Table III, although these numbers may not necessarily reflect the actual order of the higher excited states. Due to the use of different basis sets and a better optimized ground-state geometry, the T_v values and order in the present calculation are a little different from those in Ref. 10. The errors in CASPT2 computed excitation energies are typically less than 0.3 eV.[31] Double-resonance multiphoton ionization photoelectron spectroscopy[19] indicated that the first five singlet excited states of ClBz are S-A_1, S-B_2, S-A_1, S-B_2, and S-A_1,

TABLE II. The calculated and experimental frequencies (in cm^{-1}) of ClBz ground state.

Mode	Symmetry	CASSCF	CASSCF[a]	HF[a,b]	Expt.
1	a_1	3381	3009	3030	3082[c]
2	a_1	3348	2980	3016	3054[c]
3	a_1	3335	2968	2994	3031[c]
4	a_1	1714	1525	1594	1586[d]
5	a_1	1595	1420	1473	1482[d]
6	a_1	1238	1102	1154	1153[d]
7	a_1	1145	1019	1071	1093[d]
8	a_1	1079	960	999	1026[d]
9	a_1	1047	932	970	1004[d]
10	a_1	735	654	681	707[d]
11	a_1	435	387	361	417[d]
12	a_2	989	880	980	962[e]
13	a_2	784	698	970	831[e]
14	a_2	428	381	407	403[e]
15	b_1	1029	916	1002	981[e]
16	b_1	888	790	922	903[e]
17	b_1	772	687	748	741[e]
18	b_1	721	642	679	684[e]
19	b_1	510	454	470	467[e]
20	b_1	204	182	187	197[e]
21	b_2	3384	3012	3027	3096[c]
22	b_2	3355	2986	3004	3067[c]
23	b_2	1668	1485	1590	1598[d]
24	b_2	1545	1375	1435	1447[d]
25	b_2	1428	1271	1303	1327[d]
26	b_2	1253	1115	1184	1272[d]
27	b_2	1155	1028	1077	1167[d]
28	b_2	1055	939	1049	1068[d]
29	b_2	616	548	601	615[d]
30	b_2	307	273	286	295[d]

[a]Multiplied by 0.89 as recommended in W. J. Hehre, L. Radom, P. v. R. Schleyer, and J. A. Pople, *Ab Initio Molecular Orbital Theory* (Wiley, New York, 1986).
[b]Reference 27.
[c]Reference 28.
[d]Reference 29.
[e]Reference 30.

TABLE III. The MSCASPT2 vertical excitation energies (in eV) and the transition characters of the lowest singlet and triplet excited states of ClBz.

MSCASPT2			Expt.[a]	
State[b]	T_v	Transition	State	T_v
S_0-A_1	0.00		S_0-A_1	0.00
S_1-B_2	4.50	(π,π^*)	S_1-B_2	4.59
S_2-A_1	5.70	(π,π^*)	S_2-A_1	5.77
S_3-B_2	6.17	(π,π^*)	S_3-B_2	6.83
S_4-B_1	6.59	(n,σ^*)	S_4-A_1	7.02
S_5-A_2	7.19	(n,π^*)	S_5	7.58
S_6-A_1	7.50	(π,π^*)	S_6	7.71
S_7-A_2	7.53	(π,σ^*)		
S_8-B_2	7.53	(π,π^*)		
S_9-B_1	7.79	(π,σ^*)		
S_{10}-A_2	7.86	(σ,π^*)		
S_{11}-B_1	8.98	(n,σ^*)		
T_1-A_1	3.75	(π,π^*)	T_1	3.44
T_2-B_2	4.29	(π,π^*)	T_2	3.54
T_3-A_1	4.37	(π,π^*)		
T_4-B_2	5.06	(π,π^*)		
T_5-B_1	6.24	(n,σ^*)		
T_6-A_1	6.75	(π,π^*)		
T_7-B_2	6.81	(π,π^*)		
T_8-A_2	7.17	(n,π^*)		
T_9-A_2	7.46	(π,σ^*)		
T_{10}-A_2	7.63	(σ,π^*)		
T_{11}-B_1	7.64	(π,σ^*)		
T_{12}-B_1	8.34	(n,σ^*)		

[a]Reference 19.
[b]According to the present calculations, S_0 to S_6 are the first seven singlet states and T_1 to T_6 are the first six triplet states, respectively. The following five singlet and six triplet states have been labeled with consecutive subscript numbers for convenience.

respectively. The first four calculated singlet states agree with the experimental symmetry assignments. The fifth singlet state, however, is a S-B_2 state according to our calculations, in contrast to the S-A_1 experimental assignment. The calculated T_v values of the S_1-B_2, S_2-A_1, and S_6-A_1 and the T_1-A_1 excited states agree with the experimental values within the expected accuracy; see Table III. The discrepancies for the S_3-B_2, S_4-B_1, and S_5-A_2 and the T_2-B_2 excited states are somewhat larger than anticipated. This situation was not improved when we used a bigger active space and a bigger basis set including Rydberg basis, for which we see no obvious explanation. The transition character of every excited state was indicated by the present calculations and also listed in Table III.

C. CASPT2 potential-energy curves

High-quality PECs can help to provide a detailed understanding of phosphorescence and photodissociation mechanisms. This includes in particular the Franck-Condon region, which is of particular importance for much of the initial dynamics following photoexcitation. In order to study the changes in geometry of the phenyl ring for the excited states compared to the ground state, we optimized the geometries of several excited states of importance to the photodissociation processes (see Sec. IV). The geometries of S_1-B_2, S_3-B_2, T_1-A_1, and T_2-B_2 excited states were all optimized using the CASSCF method with the Cl–C_1 bond fixed at 1.746 Å which is the CASSCF optimized Cl–C_1 bond distance of the ground state; see Table I. The optimized phenyl geometries of the ground and excited states are compared in Table IV. The ring geometries of both the singlet and the triplet excited states are similar to the S_0-A_1 ground-state geometry. We also calculated the MSCASPT2 energies of these partially optimized excited states and compared these results to the vertical MSCASPT2 excitation energies, T_v,

TABLE IV. Comparison of CASSCF partially optimized phenyl geometries of the ground and excited states at the ground-state equilibrium R(Cl–C_1) bond distance (1.746 Å).

	S_0-A_1	S_1-B_2	S_3-B_2	T_1-A_1	T_2-B_2
$R(C_1-C_2)$ (Å)	1.403	1.433	1.421	1.467	1.428
$R(C_2-C_3)$ (Å)	1.399	1.437	1.525	1.362	1.437
$R(C_3-C_4)$ (Å)	1.399	1.435	1.431	1.470	1.426
Energy gap (eV)[a]	0.00	4.30	6.17	3.48	4.09
Energy gap (eV)[b]	0.00	4.50	6.35	3.75	4.29

[a]The MSCASPT2 energy difference between the excited states and ground state at their CASSCF optimized geometries.
[b]The MSCASPT2 vertical excitation energy of excited states at the CASSCF optimized ground-state geometry.

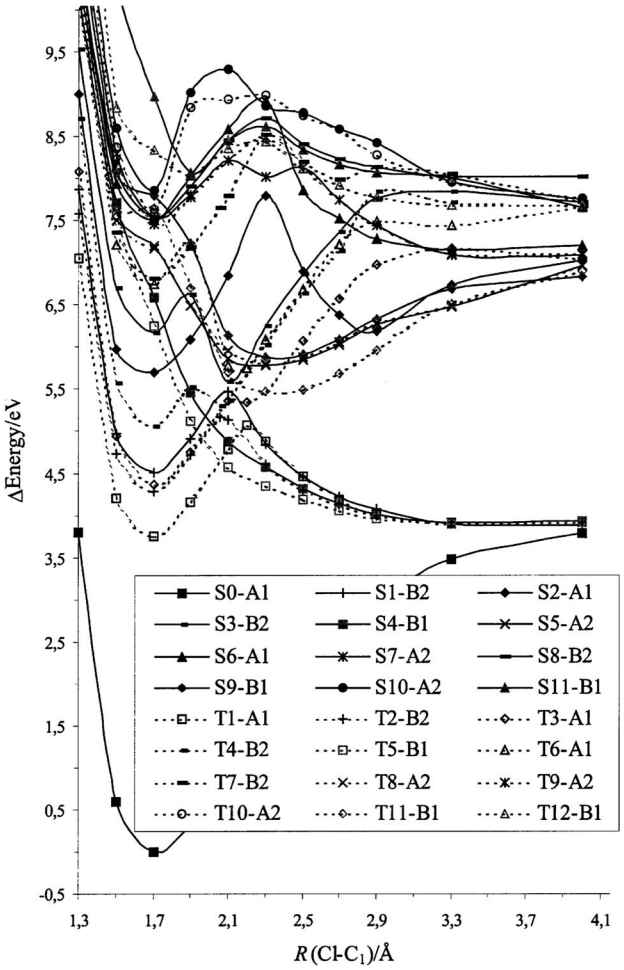

FIG. 1. MSCASPT2 adiabatic potential-energy curves along the $Cl–C_6H_5$ bond distance of 24 states of chlorobenzene. The dashed lines are used for triplet states and the solid lines are for singlet states.

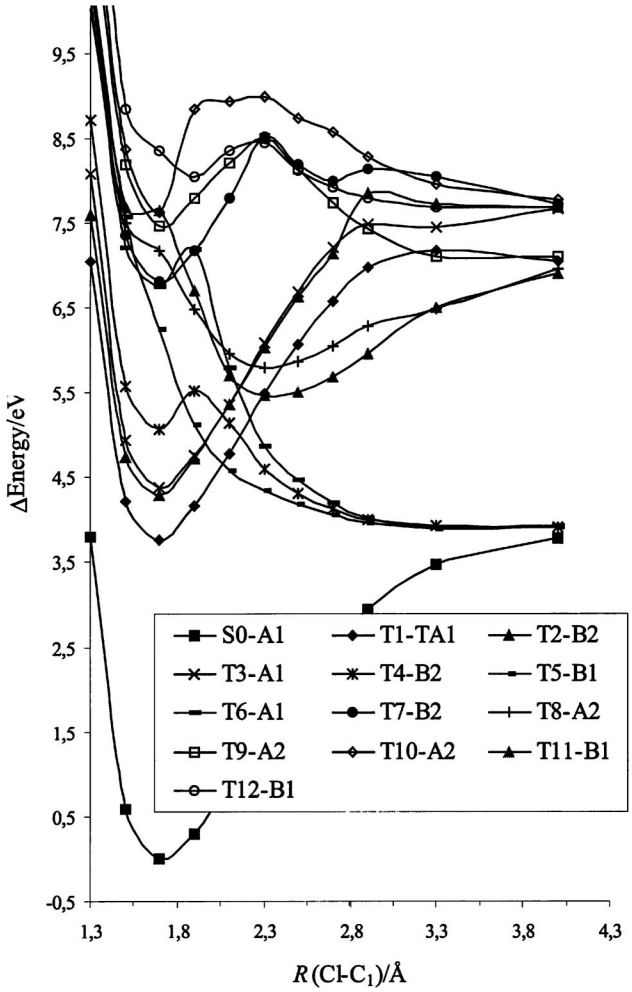

FIG. 2. MSCASPT2 diabatic potential-energy curves along the $Cl–C_6H_5$ bond distance of the singlet ground state and 12 triplet states of chlorobenzene.

for the corresponding states as calculated at the ground-state equilibrium geometry in Table IV. The resulting energy differences are less than 0.27 eV, which is less than the estimated CASPT2 error of 0.3 eV.[31] In agreement with Refs. 8 and 10, we thus conclude that optimizations of the excited states only lead to minor changes in both geometries and energies for the excited states. Moreover, optimizing the geometry of every point on the PEC of every excited state is very expensive at this high level of theory. In fact, it is nearly impossible for highly excited states. We therefore fixed the $Cl–C_1$ bond distance in steps of 0.2 Å from 1.346 to 4.046 Å and partially optimized the geometry of every point on the ground-state PEC by the CASSCF method. These geometries were subsequently used to calculate the MSCASPT2 energies of every point on the PECs of the ground and excited states, yielding MSCASPT2 PECs of the 24 states along the dissociation coordinate given by the $C_6H_5–Cl$ bond; see Fig. 1. The labels of all the states in Fig. 1 correspond to their T_v values in Table III.

IV. DISCUSSION

A. The dual phosphorescence

In order to explain the ClBz phosphorescence, we focus on the PECs of the ground state and the low-lying triplet states. In Fig. 1, there is an avoided crossing between the T_1-A_1 and T_3-A_1 states, the T_3-A_1 and T_6-A_1 states, as well as an avoided crossing between the T_2-B_2 and T_4-B_2 states. MSCASPT2 is one of the best methods currently available for calculating accurate potential-energy surfaces,[32] and the results can be used to diabatize the PECs of low-lying adiabatic states. To investigate the phosphorescence, we extracted the PECs of the ground and all the triplet states from Fig. 1 and drew them diabatically in Fig. 2. From Fig. 2, all the triplet states are bound or quasibound states except the T_5-B_1 state.

We optimized the geometries of T_1-A_1, T_2-B_2, and T_{11}-B_1 fully by the CASSCF method; see Table V. From Fig. 2 and Table V, the CASSCF optimized geometries of the T_1-A_1, T_3-A_1, T_2-B_2, and T_4-B_2 states are similar to that of the ground state. However, the CASSCF geometry of the T_{11}-B_1 state has a $Cl–C_1$ bond distance of 2.577 Å, which is 0.822 Å longer than that of the ground state. We also used MSCASPT2 to calculate the transition energies (T_e) from the T_1-A_1, T_2-B_2, T_3-A_1, T_4-B_2, and T_{11}-B_1 states to the S_0 state; see Table VI. The T_e values of the T_1-A_1 and T_3-A_1 were calculated at the CASSCF optimized geometry of the T_1-A_1 state; see Table V. The T_e values of the T_2-B_2 and

TABLE V. The calculated geometries of selected excited states (in angstrom).

	S_1-B_2			S_2-A_1	S_3-B_2	T_1-A_1		T_2-B_2	T_{11}-B_1	
Method	CAS[a]	CIS[b]	HF[c]	CAS[a]	CAS[a]	CAS[a]	HF[d]	CAS[a]	CAS[a]	HF[d]
$R(Cl–C_1)$	1.754	1.719	1.724	1.714	1.757	1.745	1.828	1.754	2.577	2.385
$R(C_1–C_2)$	1.433	1.412	1.411	1.506	1.421	1.467	1.375	1.427	1.437	1.443
$R(C_2–C_3)$	1.437	1.414	1.413	1.387	1.525	1.362	1.533	1.437	1.380	1.370
$R(C_3–C_4)$	1.435	1.413	1.412	1.499	1.431	1.470	1.386	1.426	1.420	1.416

[a]The present paper.
[b]Reference 33.
[c]Reference 15.
[d]Reference 7.

T_4-B_2 states were obtained at the CASSCF optimized geometry of T_2-B_2 state, and the T_{11}-B_1 state T_e value calculated at its CASSCF geometry are given in Table V.

The first triplet state, T_1-A_1, is a bound (π,π^*) state, and it is likely to be responsible for the slow component of the dual phosphorescence as its calculated T_e value corresponds well to the experimentally observed position of the slow phosphorescence;[11] see Table VI. This conclusion is the same as the HF calculated result in Ref. 7, and it agrees with the experimental prediction.[11] As stated in Ref. 7, the second triplet state, T_2-B_2, is also a (π,π^*) rather than a (π,σ^*) state. Moreover, according to the present calculations all the first four triplet states are (π,π^*) states; see Table III.

The first bound (π,σ^*) state included in Fig. 2 and Table III is T_{11}-B_1. As mentioned above, it has a calculated $Cl–C_1$ bond distance of 2.577 Å, which is 0.822 Å longer than that of T_1-A_1 state. This difference is about 0.6 Å in the HF calculation; see Table V. The present calculated T_e value from the T_{11}-B_1 state to the S_0 state is 2.68 eV, which is very close to the experimentally observed position of 480 nm (2.58 eV);[11] see Table VI. Therefore, we assign the T_{11}-B_1 state to be responsible for the fast part of the dual phosphorescence.[11] The T_{11}-B_1 state is the second T-B_1 state and is the same state that HF calculations assigned to the fast phosphorescence.[7]

B. Photodissociation channels of the low-lying excited states

The shortest excitation wavelength employed in the experiments was 193 nm (6.42 eV), and we therefore focus mainly on the excited singlet states with T_v under or near 193 nm and the repulsive triplet states which are likely to interact with these singlet states. These are the S_0-A_1, S_1-B_2, S_2-A_1, S_3-B_2, S_4-B_1, and T_5-B_1 states. There is one avoided crossing between S_1-B_2 and S_3-B_2. We extracted the PECs of these states from Fig. 1 and drew them diabatically; see Fig. 3. From Fig. 3 and Table III, S_1, S_2, and S_3 are bound (π,π^*) states, whereas S_4 and T_5 are repulsive (n,σ^*) states.

TABLE VI. The MSCASPT2 transition energies of several triplet states to S_0 state.

Transition	MSCASPT2[a] (eV)	The dual phosphorescence positions experimentally observed[b]
$S_0 \leftarrow T_1$-A_1	3.10	≈400 nm (3.10 eV)
$S_0 \leftarrow T_2$-B_2	4.04	
$S_0 \leftarrow T_3$-A_1	4.68	
$S_0 \leftarrow T_4$-B_2	4.96	
$S_0 \leftarrow T_{11}$-B_1	2.68	≈480 nm (2.58 eV)

[a]The T_v value of the T_3-A_1 state was calculated at the CASSCF geometry of the T_1-A_1 state, and the T_v value of the T_4-B_2 state was calculated at the CASSCF geometry of the T_2-B_2 state.
[b]Reference 11.

S_4-B_1, with 6.59-eV T_v, is the highest singlet excited state that the photon of 193-nm (6.42 eV) wavelength used experimentally[16–18] could reach. It is a repulsive state, which will dissociate directly on a very short time scale.[34] This direct dissociation should contribute to the fastest of the three channels observed in Ref. 16. The CASSCF optimized geometries of the first three singlet excited states were listed in Table V. As shown in Fig. 3, S_3-B_2 is a quasibound state with a barrier that blocks immediate dissociation. The energy gap between its saddle point and the minimum of the ground state is about 6.6 eV. It is possible that molecules excited with photons with a wavelength of 193 nm can overcome the predissociation barrier if the MSCASPT2 error of 0.3 eV is taken into account. If so, its lifetime will depend on the tunneling rate. This process would proceed as a so-called vibrational or Herzberg's type II predissociation.[35] This fast predissociation could then also contribute to the fastest dissociation channel as proposed in Ref. 16. From Fig. 3, the PEC of S_3-B_2 crosses the repulsive (n,σ^*) T_5-B_1 state. The $Cl–C_1$ bond distance at the crossing point is about 1.82 Å. It is also about 0.2 eV lower than 193 nm. So, we assign the second experimentally observed channel as the intersystem crossing from the bound (π,π^*) S_3-B_2 state to the repulsive (n,σ^*) T_5-B_1 state. The complex will ultimately decay with a rate that depends on the coupling between the two electronic states. This is an electronic predissociation process, which is also called a Herzberg's type I predissociation.[35] The third photodissociation channel is slower than the first two channels[16] and was suggested to take place via internal conversion to highly excited vibrational levels of the ground state (hot molecule).[16] From Fig. 3, it appears likely that the S_3-B_2 state first undergoes internal conversion to the S_1-B_2 state. The lowest vibrational state of S_1 is much closer in energy to the dissociation limit of S_0, and thereby makes international conversion from S_1 to S_0^* more likely. This mechanism is compatible with the third observed photodissociation channel with lower rate.

The highest singlet excited state the photon with 248-nm (5.00 eV)[16] wavelength can reach is S_1-B_2, whose T_v is 4.50 eV. S_1 is a bound (π,π^*) state, which cannot dissociate by itself. However, the S_1-B_2 state can undergo an intersystem

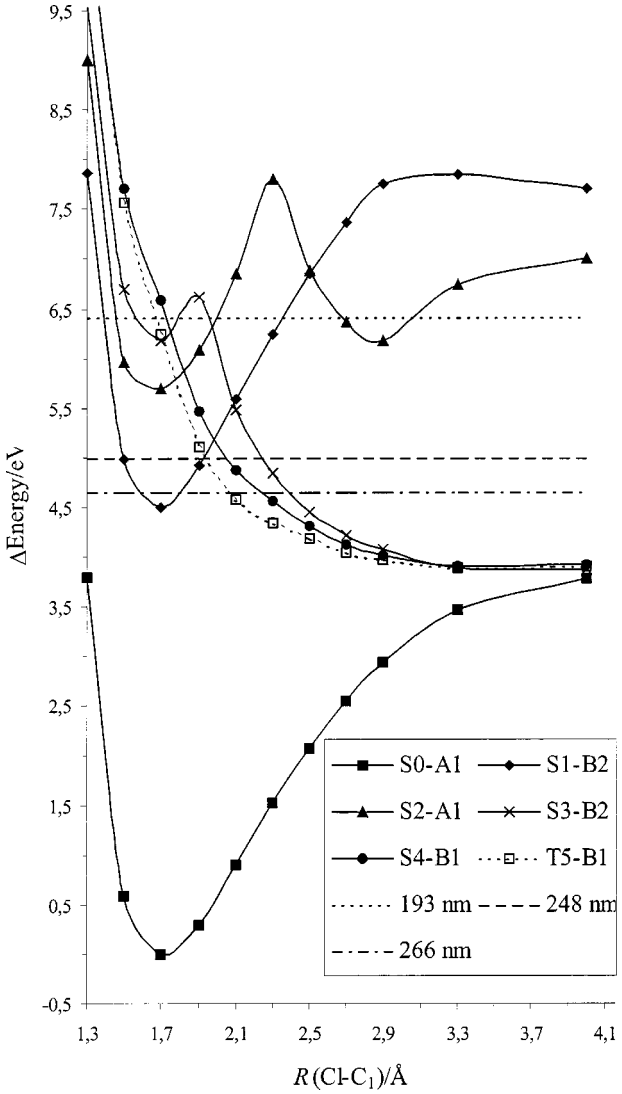

FIG. 3. MSCASPT2 diabatic potential-energy curves along the $Cl–C_6H_5$ bond distance of one triplet and five singlet states of chlorobenzene. The horizontal dashed lines indicate the 193-, 248-, and 266-nm excitation energy used in previous experiments.

crossing to the repulsive (n,π^*) T_5-B_1 state. The $Cl–C_1$ calculated bond distance at the crossing point is about 2.02 Å. The energy gap between this point and the minimum of the ground state is about 5.0 eV. The complex will ultimately decay due to spin-orbit coupling between the two electronic states. So, the first channel of photodissociation of ClBz at 248 nm is the intersystem crossing from S_1-B_2 to T_5-B_1, and it is a Herzberg's type I predissociation.[35] From Fig. 3, the PEC of S_1-B_2 also undergoes an internal conversion with the repulsive (n,π^*) S_4-B_1 state. The $Cl–C_1$ bond distance at the crossing point is about 2.06 Å. The energy gap between this point and the minimum of the ground state is about 5.15 eV. If the 248-nm-wavelength photon used in the experiment overcomes this energy barrier, then the complex will ultimately decay by internal conversion. So, the first channel of photodissociation of ClBz at 248 nm is also possibly via the internal conversion from S_1-B_2 to S_4-B_1. The second slower photodissociation channel observed experimentally is again possibly dissociation via the highly vibrational levels of the ground state, S_0^*. As discussed above, S_0^* could be produced by internal conversion from the S_1 state.

The 266-nm (4.66 eV) -wavelength photon can also reach the S_1-B_2 state. As with the 248-nm excitation, this state cannot dissociate by itself. The PEC of S_1-B_2 crosses to the PECs of T_5-B_1 and S_4-B_1 states. The photoexcitation energies required to reach these two crossing points are about 5.0 and 5.25 eV, respectively. The 266-nm (4.66 eV) -wavelength photon is unlikely to reach either of the two points, even considering an estimated error of 0.3 eV, just as we said before.[10] If the predissociation channels are out of reach, the only remaining photodissociation channel at 266 nm is again via the highly vibrational levels of the ground state, S_0^*, produced by the internal conversion from the S_1 state, as discussed above. Both Refs. 15 and 5 indicated that the photodissociation following 266-nm excitation is slow, even though the latter assigned it to the decay of an initially excited (π,π^*) state to a repulsive triplet (n,σ^*) state due to spin-orbit coupling.

V. CONCLUSIONS

In order to explain the dual phosphorescence and the photodissociation mechanism of chlorobenzene at 193, 248, and 266 nm, we calculated MSCASPT2 potential-energy curves of 24 singlet and triplet states. The bound (π,π^*) T_1-A_1 state is responsible for the slow part of the dual phosphorescence, and the bound (π,σ^*) T_{11}-B_1 state will be responsible for the fast part of the dual phosphorescence. The photodissociation of chlorobenzene at 193 nm has three channels: (1) a direct dissociation of the repulsive (n,σ^*) S_4-B_1 state, or Herzberg's type II predissociation as the quasibound (π,π^*) S_3-B_2 state dissociates by tunneling, (2) Herzberg's type I predissociation arising from an intersystem crossing from the quasibound (π,π^*) S_3-B_2 state to the repulsive (n,σ^*) T_5-B_1 state, and (3) via highly vibrational levels of the ground state, which are produced from S_1-B_2 state by internal conversion after its internal converting with the S_3-B_2 state. For chlorobenzene photodissociation at 248 nm, there are two channels: (1) Herzberg's type I predissociation arising from an intersystem crossing from quasibound (π,π^*) S_1-B_2 state to repulsive (n,σ^*) T_5-B_1 state, or internal conversion from (π,π^*) S_1-B_2 state to repulsive (n,σ^*) S_4-B_1 state, and (2) via highly vibrational levels of the ground state, which are produced from S_1-B_2 state by internal conversion. However, the photodissociation of chlorobenzene at 266 nm has only one channel, which is via highly excited vibrational levels of the ground electronic state.

ACKNOWLEDGMENTS

The Swedish Research Council (VR) and the Magnus Bergvall Foundation are gratefully acknowledged for financial support. The Swedish National Supercomputer Center (NSC) is acknowledged for generous grants of computer resources. The authors wish to thank Dr. Chi-Kung Ni and Professor KeLi Han for helpful discussions about the photodissociation channels.

[1] T. Matsuura and K. Omura, Bull. Chem. Soc. Jpn. **39**, 944 (1996).
[2] J. S. Zhang, T. T. Miau, and Y. T. Lee, in *XIVth International Symposium on Molecular Beams* (Lawrence Berkely Lab, 1992), pp. 29–31.
[3] P. Y. Cheng, D. Zhong, and A. H. Zewail, Chem. Phys. Lett. **237**, 399 (1995).
[4] T. Okutsu, T. Kageyama, N. Kounose, J. Tsuchiya, and H. Hiratsuka, Chem. Phys. Lett. **299**, 597 (1999).
[5] M. Kadi, A. N. Tarnovsky, M. Rasmusson, J. Davidsson, and E. Åkesson, Chem. Phys. Lett. **350**, 93 (2001).
[6] H. Zhang, R.-S. Zhu, G.-J. Wang, K.-L. Han, G.-Z. He, and N.-Q. Lou, J. Chem. Phys. **110**, 2929 (1999).
[7] S. Nagaoka, T. Takemura, H. Baba, N. Koga, and K. Morokuma, J. Phys. Chem. **90**, 759 (1986).
[8] M. Rasmusson, R. Lindh, N. Lascoux, A. N. Tarnovsky, M. Kadi, O. Kuhn, V. Sundström, and E. Åkesson, Chem. Phys. Lett. **367**, 759 (2003).
[9] Y.-J. Liu, P. Persson, H. O. Karlsson, S. Lunell, M. Kadi, D. Karlsson, and J. Davidsson, J. Chem. Phys. **120**, 6502 (2004).
[10] Y.-J. Liu, P. Persson, and S. Lunell, J. Phys. Chem. **108**, 2339 (2004).
[11] T. Takemura, Y. Yamada, and H. Baba, Chem. Phys. **68**, 171 (1982).
[12] T. Takemura, Y. Yamada, M. Sugawara, and H. Baba, J. Phys. Chem. **90**, 2324 (1986).
[13] O. Rubio-Pons, O. Loboda, B. Minaev, B. Schimmelpfenning, O. Vahtras, and H. Ågren, Mol. Phys. **101**, 2103 (2003).
[14] J. Finley, P.-Å. Malmqvist, B. O. Roos, and L. Serrano-Andrés, Chem. Phys. Lett. **288**, 299 (1998).
[15] G.-J. Wang, R.-S. Zhu, H. Zhang, K.-L. Han, G.-Z. He, and N.-Q. Lou, Chem. Phys. Lett. **288**, 429 (1998).
[16] T. Ichimura, Y. Mori, H. Shinohara, and N. Nishi, Chem. Phys. **189**, 117 (1994).
[17] T. Ichimura, Y. Mori, H. Shinohara, and N. Nishi, Chem. Phys. Lett. **122**, 51 (1985).
[18] A. Freedman, S. C. Yang, M. Kawasaki, and R. Bersohn, J. Chem. Phys. **72**, 1028 (1980).
[19] P. Asselin, F. Piuzzi, M. Mons, and I. Dimicoli, Chem. Phys. **191**, 261 (1995).
[20] K. Andersson, M. Barysz, A. Bernhardsson *et al.*, MOLCAS version 5.4 (University of Lund, Sweden, 2000).
[21] K. Pierloot, B. Dumez, P.-O. Widmark, and B. O. Roos, Theor. Chim. Acta **90**, 87 (1995).
[22] M. Head-Gordon, J. A. Pople, and M. J. Frisch, Chem. Phys. Lett. **153**, 503 (1988).
[23] W. J. Hehre, L. Radomr, P. V. R. Schleyer, and J. A. Pople, *Ab Initio Molecular Orbital Theory* (Wiley, New York, 1986).
[24] M. J. Frisch, G. W. Trucks, H. B. Schlegel *et al.*, GAUSSIAN 03, Revision A.1, Gaussian, Inc, Pittsburgh PA, 2003.
[25] S. Cradock, J. M. Muir, and D. W. H. Rankin, J. Mol. Struct. **220**, 205 (1990).
[26] P. Imhof and K. Kleinermanns, Chem. Phys. Lett. **270**, 227 (2001).
[27] T. G. Wright, S. I. Panov, and T. A. Miller, J. Chem. Phys. **102**, 4793 (1995).
[28] D. H. Whiffen, J. Chem. Soc. 1350 (1956).
[29] H. D. Bist, V. N. Sarin, A. Ojha, and Y. S. Jain, Spectrochim. Acta, Part A **26**, 841 (1970).
[30] Y. S. Jain and H. D. Bist, J. Mol. Spectrosc. **47**, 126 (1973).
[31] M. Merchan, L. Serrano-Andres, M. P. Fülscher, and B. O. Roos, in *Recent Advances in Multireference Theory*, edited by K. Hirao (World Scientific, Singapore, 1999), Vol. IV, pp. 161–196.
[32] H. Nakamura and D. G. Truhlar, J. Chem. Phys. **118**, 6816 (2003).
[33] D. M. Upadhyay, M. K. Shukla, and P. C. Mishra, J. Mol. Struct.: THEOCHEM **531**, 249 (2000).
[34] R. Schinke, *Photodissociation Dynamics* (Cambridge University Press, Cambridge, 1993).
[35] G. Herzberg, *Spectra of Polyatomic Molecules*, Molecular Spectra and Molecular Structure III (Van Nostrand, New York, 1967).